

Sudden modulation in the UHF wireless signals probably caused by the activation of pre-earthquake processes. Case studies for the Balkans (SE Europe)

Dimitar Ouzounov^{*,1}, Sylvia Velichkova-Yotsova², Sergey Pulinetz³

⁽¹⁾ Institute for Earth, Computing, Human and Observing (Institute for ECHO), Chapman University, Orange, CA, USA

⁽²⁾ National Institute of Geophysics, Geodesy and Geography, Sofia, Bulgaria

⁽³⁾ Space Research Institute, Russian Academy of Sciences, Moscow, Russia

Article history: received June 1, 2023; accepted December 22, 2023

Abstract

We study the atmospheric variations of broadband wireless signal propagation intensity correlated with pre-earthquake processes. We have maintained ground observations in the VHF range of 1.8 and 3.5 GHz in Bulgaria (Southeast Europe), close to the border with Greece and Northern Macedonia, since 2012. The signal source is 1.8 GHz –LTE broadcasting cellular communication signal and the receivers are digital HF to SHF antennae collecting the data via mobile internet. Our observations revealed phenomena associated with a natural enhancement of the intensity of the signals (no change in the transmitting level) days/hours before the seismic events, even far from the observation region. We are presenting the results for four significant earthquakes in the area: (1) M5.6 on May 22, 2012, in Bulgaria, (2) M6.9 on May 24, 2014, in the Aegean Sea, Greece, (3) M6.5 on Nov 17, 2015, Lefkada, Greece, and (4) M6.3 of May 12, 2017, in Western Türkiye. Some changes in the atmospheric boundary layer (ABL), triggered by an intensification of radon and other released gases, could lead to a change in lower atmospheric conductivity. Although the intensity modulation was observed far (> 200 km) from the epicenter areas, the anomalies were always inside the estimates of the Dobrovolsky-Bowman area of preparation. We examined the possible correlation between magnitude and the spatial size of the earthquake preparation zone in the Lithosphere-Atmosphere-Ionosphere coupling (LAIC) framework.

Keywords: Earthquake precursors; UHF; VHF; LAIC; Ionization; Radon

1. Introduction

For the last 15 years, considerable progress in the physical understanding of the pre-earthquake processes has been achieved [Pulinetz and Ouzounov, 2011; Pulinetz et al., 2015; Ouzounov et al., 2018; Pulinetz et al., 2018]. It was revealed that substantial modification of the near-the-surface Atmosphere boundary layers (ABL) layer of the atmosphere occurs under increased geo-gases (radon, methane, CO₂) released during the earthquake preparation processes. The primary energy driver is the ionization produced by radon decay and the release of

energetic alpha particles with an energy of ~ 5.6 MeV. This modification is expressed mainly by changes in the air's electrical properties due to the variation of its conductivity (increase/decrease) during different phases of ion-induced nucleation. All these launch the cascade type of processes, creating anomalies in the troposphere and ionosphere, which other techniques could observe. The chain of processes existed shortly (weeks/ few days) before the earthquake's occurrence. These pre-earthquake processes have synergetic behavior, a typical signature for open dissipative systems [Knyazeva and Kurdyumov, 2003]. The first observation of atmosphere/ionosphere in the Very High-Frequency range (VHF) concerning earthquake processes was established in Japan during two major projects on seismo-electromagnetics: (a) RIKEN (Institute of Physical and Chemical Research) and (b) NASDA (National Space Development Agency of Japan, (now is named JAXA) in the Earthquake Integrated Frontier framework of the Science and Technology Agency (now MEXT) during 1996-2001. The RIKEN project was led by S. Uyeda, and the NASDA project by M. Hayakawa [Hayakawa, 2018; Uyeda and Nagao, 2018]. During the NASDA project, the ground- and satellite-based observations were expanded toward atmospheric and ionospheric signatures of earthquakes [Fukumoto et al., 2001; Kushida and Kushida, 2002]. The over-the-horizon VHF (30-300 MHz) transmitter signals were observed before many earthquakes in Japan, and their direction-finding results suggested that the existence of those signals is very likely caused not by ionospheric reflection but by atmospheric perturbations. Statistical study of pre-earthquake VHF phenomena was conducted by Fujiwara et al. [2004], Yonaiguchi et al. [2007], and Yasuda et al. [2009] further extended this VHF study by developing a new interferometric direction finder. This new finder enabled the separation of the natural VHF pre-earthquake noises and over-the-horizon VHF signals. Moriya and his team from Hokkaido University established an extensive network for the over-the-horizon VHF signals (70-90 MHz) at many stations in Hokkaido, and Moriya et al. [2010] have made a statistical study based on the long-term data on the over-the-horizon VHF radio signals and found a close correlation of VHF signals with earthquakes. Finally, we can add that VHF network observation has also continued in Greece [Kapiris et al., 2002].

2. Materials and method

The observations in the UHF and SHF range as part of our research to validate the Lithosphere-Atmosphere-Ionosphere Coupling (LAIC) concept concerning earthquakes started in 2012 with test observations of continuously recording data in the VHF range. The initial observation in May 2012 in Bulgaria coincided about a month ahead of the seismic activities near Sofia (Bulgaria) associated with the M5.6 earthquake near Pernik (NW Bulgaria). The initial data analysis revealed a phenomenon related to the sudden enhancement of the intensity in the range of 3.5 GHz signals days before the time of seismic occurrence. During this period, the intensity variations in 3.5 GHz signals have been studied with WiMAX technology correlated with earthquake preparation processes [Ouzounov et al., 2019].

The SHF observation continued with the WiMAX modem in Bulgaria until 2015, and the accumulated data show common changes in the atmosphere over the regions of ongoing earthquake preparation, like Moriya et al., [2010], based only on VHF-band radio wave propagation. Since 2015, the frequency range in observations has been updated in the UHF and SHF range of 1.8-3.5 GHz for two receiving sites located in SW Bulgaria (EU).

In this paper, we present the results from the observational site located in SW Bulgaria (SE Europe) close to the border with Northern Greece and Northern Macedonia (Figure 1, Table 1). Since 2016, the UHF observations have been conducted with EMC antennas (Aaronia-VHF) with receiving range 10 MHz-6 GHz and real-time processing RF Spectrum Analyzer with Displayed Average Noise Level DANL: -135 dBm (1 Hz). During the observation, a period was reported for more than 15 cases of $-$ pre-earthquake influence on UHF wireless signals for seismic events at different distances (30-260 km) and within the magnitude range M3.5-M6.5 [Ouzounov et al., 2016, 2017, 2019, 2021]. The data analysis of UHF observations revealed a natural enhancement of the intensity of the signals (no change in the transmitting level) days/hours before the seismic events, even far from the observation region. In this paper, four significant earthquakes in the region have been analyzed: (1) M5.6 on May 22, 2012, in Bulgaria, (2) M6.9 on May 24, 2014, in the Aegean Sea, Greece, (3) M6.5 on Nov 17, 2015, Lefkada, Greece, and (4) M6.3 of May 12, 2017, in Western Türkiye (Figure 1, Tables 2,3).

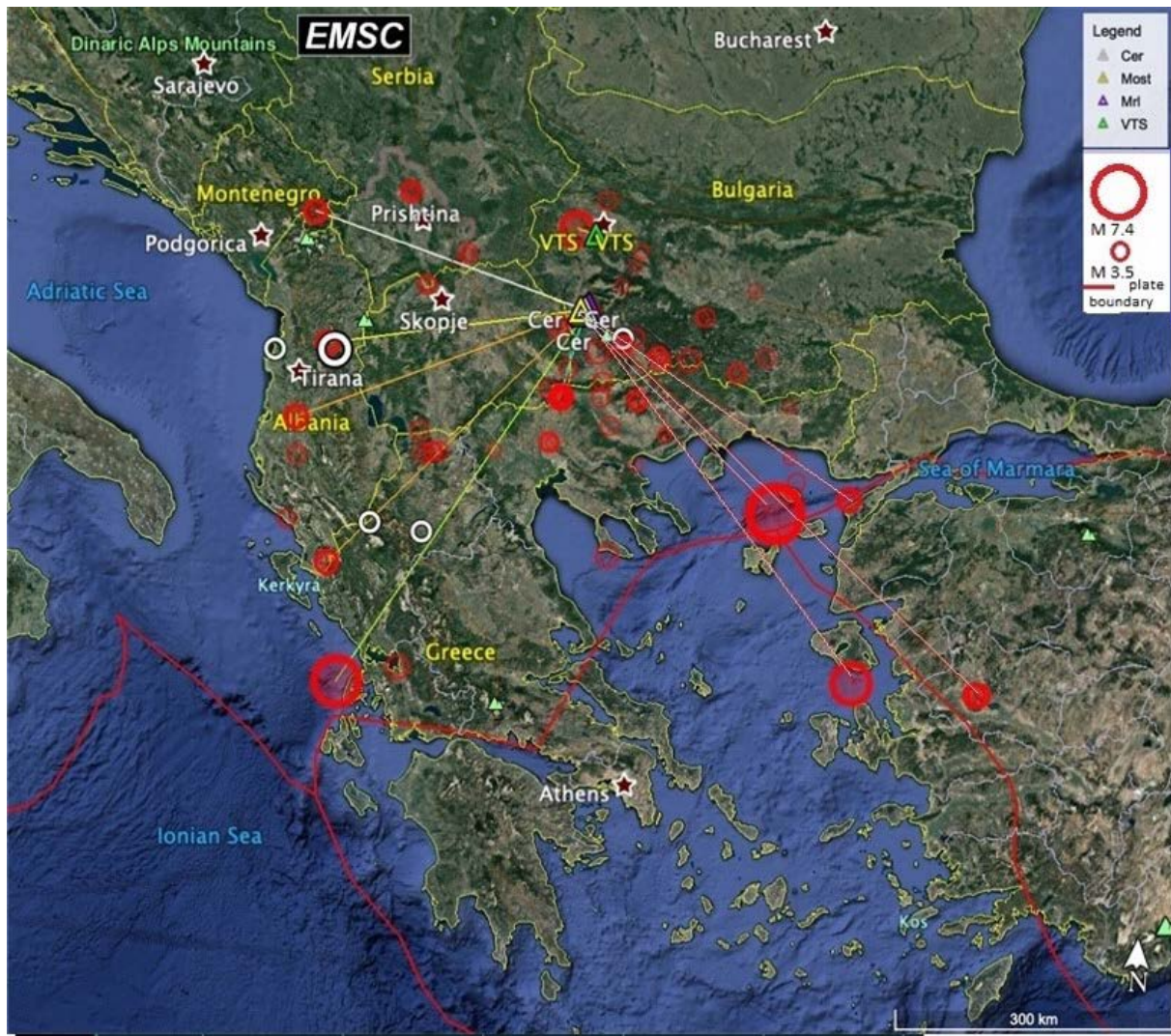


Figure 1. Reference map of Balkans and SW Bulgaria, with the locations of the analyzed earthquakes. A green triangle shows the VTS station, with the yellow triangle Cerovo transmitter and the location of MOZ and MAR receivers.

2.1 Observation methodology

The monitoring of the anomalous increase of the high-frequency Internet signal started in Bulgaria in 2012 near the capital, Sofia, in the area of Golden Bridges-Vitosha Park, about 1395 m above sea level (asl). The first observation was just with non-regular tests computing the average of the prevailing daily signal level. A Huawei B-315 modem software with a 3.5 GHz-WiMax analog wireless Internet modem has been used. The transmitter was located at 8 km WNW under the peak Dupevitsa in the Lyulin Mountain – about (1104 m asl).

In June 2013, regular signal observations with the same modem began in SW Bulgaria at site Moshtanets (MOS) near the border with FYR and Greece at 470 m above sea level. Observations started with several series of video AVI recordings of 5-10 minutes per day and later – with continuous 24-hour AVI recording of the modem signal level with numerical values of the level in dBm – input/output signal in dB. The monitoring of SHF (3.5 GHz) signal modulation continued under the same scheme until August 2014, when the 1.8 GHz –LTE technology became available for use. In October 2014, observations continued with a digital VHF Directional antenna based on SPECTRAN NF equipped with the Aaronia REAL 3D (isotropic) magnetic field sensor, which provides recording in the range of 500-4500 MHz.

In 2015, observations continued with the addition of a second Aaronia antenna at site Marulovo (MAR)-about 845 m above sea level on the other side of the primary fault system (Figure 2). Both antennas at sites MAR and MOS have been recording signals from the same transmitter located at Tserovo, about 719 meters from the sea level. The transmitter directions to the two stations are approximately perpendicular to each other. The distance between MAR and MOS is about 4-5 km.

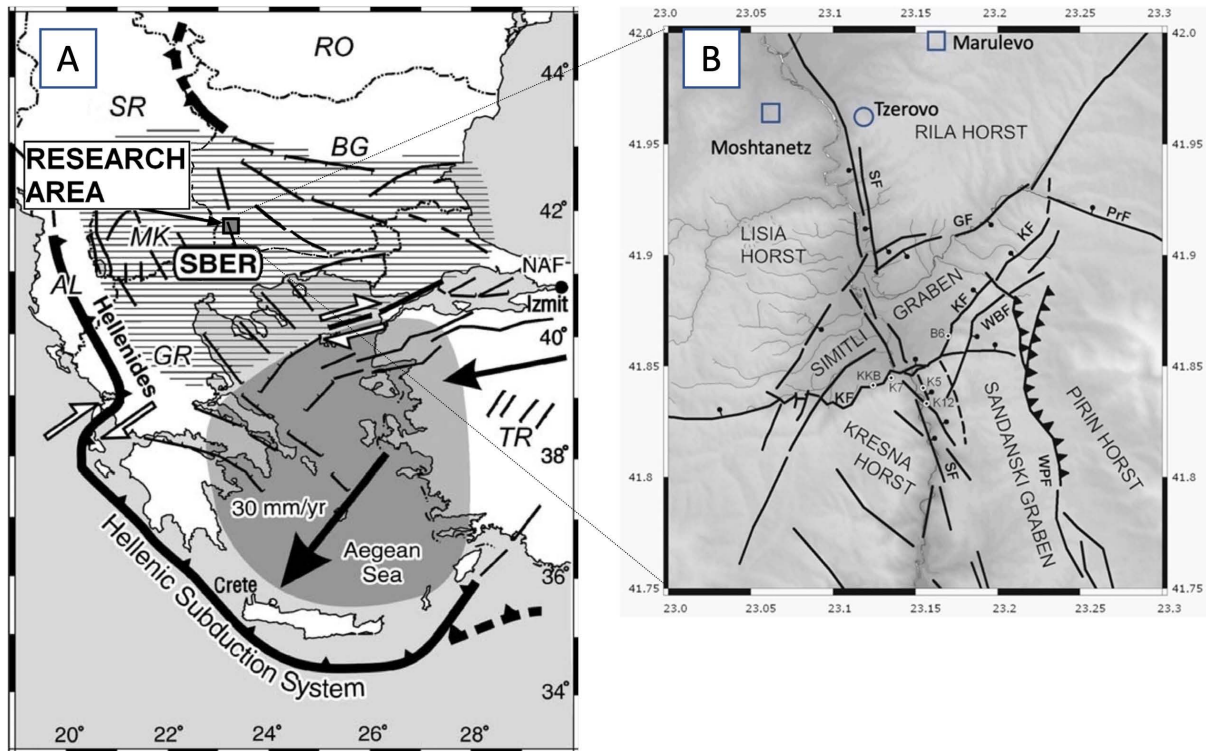


Figure 2. A: Simplified tectonic map of the eastern Mediterranean with research area [adapted from McClusky et al., 2000; Kotzev et al., 2006]. The Grey quadrangle shows the research area. Hatching shows the South Balkan extensional region (SBER). The shaded area indicates the supra-subduction extensional region. Countries: AL, Albania; BG, Bulgaria; SR, Serbia; GR, Greece; MK, FYR of Macedonia; RO, Romania; TR, Türkiye. More details in Dobrev [2011]. B: A simplified sketch showing the main tectonic structures in the observation area. The observation points MAR, MOS, and the transmitter Tserovo are also shown. After [Dobrev, 2011].

Based on the first year of digital recording, we have found a significant increase in the number of pulses with amplitudes above average before the earthquakes of M3.5 to M6.9. The different durations of the pulses are proportional to the magnitude M and inversely proportional to the distance to the epicenter of the earthquakes. The aim of continuing the observation is to study the relationships between the number and duration of pulses as a function of magnitude/distance/time since the occurrence of earthquakes. Enumeration of pulses for determining the frequency distribution of the VHF signal is performed according to the following methodology (Figure 3):

- 1) The signal source is 1.8 GHz –LTE transmitter towers broadcasting as part of Bulgaria’s standard cellular communication network.
- 2) The receivers are digital Aaronia-VHF to SH directional antenna collecting the data via mobile internet (Figure 3).
- 3) Lists the impulses for each hour of recording by the waterfall channel or by the total day log recording channel (Figure 3C). The amplitudes should be above the setpoint of 50 dBm.
- 4) It is selected so that pulses from frequencies other than the operating frequency – 1.7-1.8 GHz – are not recorded in the total recording.
- 5) In cases where noise with higher amplitudes is noisy, the waterfall channel eliminates unnecessary impulses outside the operating frequency range. The recording settings are tailored for higher accuracy.

2.2 Atmospheric Chemical Potential (ACP)

All thermodynamic models of the atmosphere, considering the phase transitions of water and latent heat fluxes, operate with latent heat (per mole or molecule) as a constant at a given temperature. It is equal to 0.422 eV per one water molecule. We observed additional variations in temperature, humidity, and pressure when studying the processes of ionization of the surface manner layer of the atmosphere by radon, the release of which from the

Modulation in the UHF signals caused by pre-earthquake processes

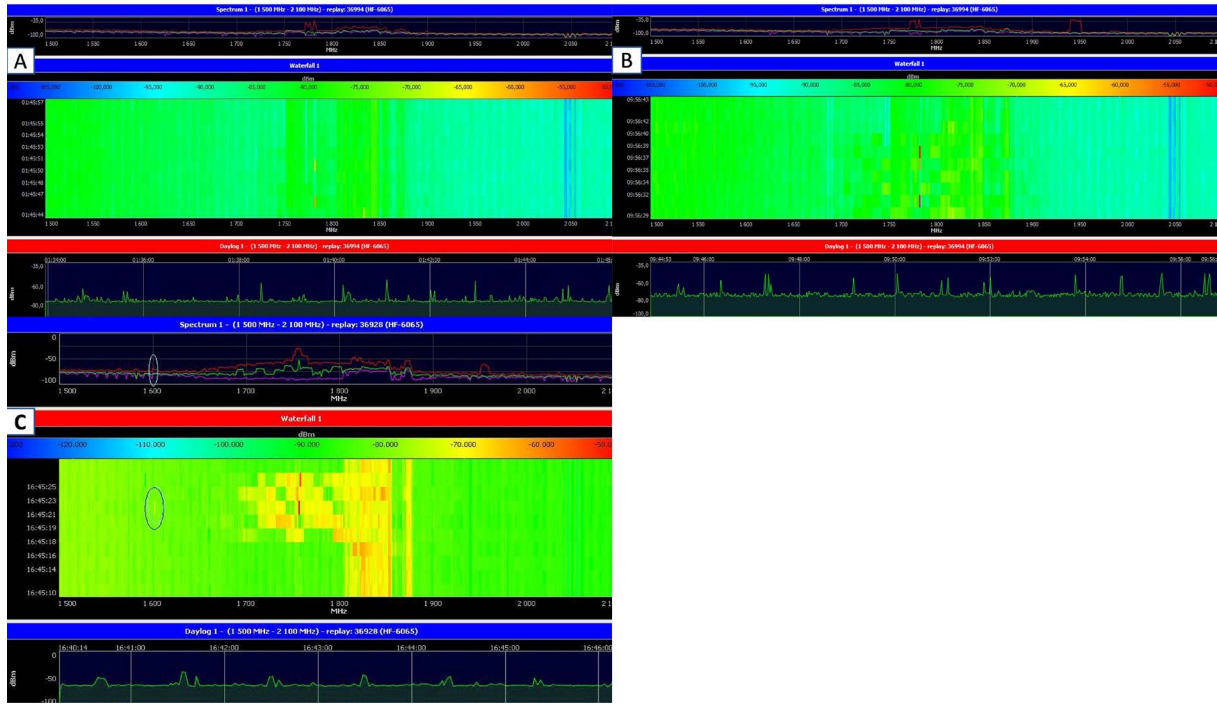


Figure 3. Typical analysis with Aaronia-UHF directional antenna. Three different types of analyses have been used: spectral analysis (upper panel), spectral Falls (middle panel), and time series (bottom panel). A: Recording of the calm atmospheric environment on May 14, 2017; B: Recording of the disturbed atmospheric environment on May 27, 2017; C: Recording of lightning flashes from the observational antenna on June 10, 2018. The effects of storms and lightning are easily quantified because they occur in a wide frequency range (1.6-2.5 GHz) and with relatively constant amplitude modulation.

Earth's crust sharply increases at the final stage of preparation for a strong earthquake [Pulinets et al. 2006]. The detailed calculations are in Pulinets et al. [2006; 2018]. It turned out that the released amount of latent heat is more significant at a high rate of ion production and high concentration of ions than for ordinary condensation. For earthquakes, the value ranges from 0.01 to 0.1 eV, i.e., in extreme cases, it can reach about 25% of the latent heat constant (it is the difference between the released latent heat during hydration and normal condensation). We call it the atmospheric chemical potential (ACP) because, in evaporation/condensation, the energy of the water molecule is equal to its chemical potential. Although we only use air temperature and relative humidity for calculation, it reflects the effects of radon ionization on the ABL of the atmosphere, changing its thermodynamic and electric properties.

2.3 Earthquake Preparation Zone

Various authors developed the concept of an earthquake preparation zone [Dobrovolsky et al., 1979; Keilis-Borok and Kossobokov, 1990; Bowman et al., 1998]. In general terms, it is an area where local deformations connected with the source of the future earthquake are observed. Naturally, the deformations imply changes in the crust properties accompanied by different geophysical anomalies, which various geophysical monitoring techniques can measure. According to Dobrovolsky et al. [1979], the empirical relation to determining the size of the earthquake preparation zone (EPZ) is given by:

$$R = 10^{0.43M} \text{ km.} \quad (1)$$

R is the EPZ radius in kilometers, and M is the earthquake's magnitude.

Bowman et al. [1998] consider the critical earthquake concept to be an earthquake acceleration process while the system approaches the critical point. Earthquake activation zone-R is linearly related to the most significant fault within the activated fault system. But R is nearly ten times larger than the length of the largest activated fault and can be estimated as

$$R = 10^{0.44M} \text{ km} \quad (2)$$

where R is the EPZ radius in kilometers, and M is the earthquake’s magnitude. Table 1 shows the EPZ size calculated for different magnitudes.

Magnitude	3	4	5	6	7	8	9
Earthquake preparation zone radius R (km)	19.5	52.5	141	380	1022	2754	7413

Table 1. EPZ radius for different magnitudes according to the Dobrovolsky formula (Eq. 1).

We are analyzing two physical parameters characterizing the state of development in the ABL during earthquakes shown in Table 1. (i) Monitoring of propagation intensity of VHF wireless signals in ranges of 1.8-3.5 GHz and (ii) computed ACP from ground and satellite observations. This approach provides a complex view of the scale and physics of changes in the atmospheric processes related to tectonic activity. To understand the day-by-day variability of ACP during earthquake events, we analyzed three hours of global ACP data computed from the GEOS-5 assimilation [Pulinets et al., 2022; Ouzounov et al., 2021]. We use Dobrovolsky-Bowman estimates of EPZ where the radius (Table 1) scales exponentially with earthquake magnitude and gives an extended coverage to examine VHF anomalies.

3. Results

#	Region	Date	Time [UTC]	Long, E/ Lat, N	Depth [km]	Magnitude	Focal mechanism	Distance to VHF receiver [km]	Dobrovolsky-Bowman area radius [km]	Freq Range [GHz]	Time lag [h]	Number of impulse changes
1	ALBANIA	2018-08-11	15:38:34.0	41.59/20.21	10	Mw = 5.1	strike-slip-normal fault	65/45	156	1.8	48	30
2	BULGARIA	2018-08-02	14:17:37.6	41.69/23.59	10	ML = 4.1	strike-slip-normal fault	50/30	58	1.8	96	80
3	NORTHERN GREECE	2018-01-02	04:24:16	41.22/22.86	6	mb = 5	oblique normal	85	141	1.8	114	39
4	COAST OF W. TURKEY	2017-06-12	12:28:37	38.85/26.31	9	Mw = 6.3	oblique normal	437	512	1.8	560	42
5	GREECE-near Lefkada	2015-11-17	07:10:08	38.76/20.45	10	Mw = 6.5	strike-slip	420	624	1.8	267	34
6	AEGEAN SEA	2014-05-24	09:25:02	40.29/25.4	27	Mw = 6.9	strike-slip (right)	266	927	3.5/AVI	2000	10
7	BULGARIA-near Sofia	2012-05-22	00:00:33	42.66/23.01	10	Mw = 5.6	normal	19	256	3.5	120	7.5

Table 2. The earthquake catalog (source EMSC catalog) for the period of 2012-2018 was analyzed with VHF observations and shown in Figure 1.

3.1 Variations in the radio signal of 3.5 GHz preceding the earthquake of M 5.8, May 22, 2012, Pernik, NW Bulgaria

Signal observations in North West Bulgaria began in January 2012. Meteorological conditions for the entire observation period to date have no apparent impact on the quality and signal level. For the whole observation period – January-October 2012, about 270 days – an anomalous strong signal appeared only about 10-15 days-five days before and ten days after the earthquake (Figure 4). The antenna transmitters for mobile internet 3.5 G technology with a frequency of 3.5 GHz and power of 10 watts is located at Mountain Vitosha, 12-15 km away from the receiver.

On May 20, 2012, the signal suddenly became very strong, and it remained maximally strong (100% for receiver range) until May 25, 2012. Then, the signal becomes inconsistent for the next day. After the May 22nd main shock, the subsequent shocks caused the same type of anomaly. A new anomalously high signal value was recorded again on Jan 19, 2013, two days after an earthquake with M 2.8-2.9 40 km away from observations was registered. The receiver’s scope is of a constant, not a dynamic range, conditionally divided (on a linear scale) by 10 degrees. In the “relaxed” period, the signal is from 0 to 3, predominantly 2. The transmitter (antenna of Lyulin Mountain) transmits a spherically radiated signal at a frequency of 3.5 GHz and a signal power of 5-10 W in a relatively isotropic environment. The signal is amplified further when the layer (1400 m height) is excited with high conductivity. Whatever the power is of the radiated signal, the distance to which it is pierced is slightly more than 10 km. The base here is much shorter than the ionosphere studies made by [Moriya et al. 2010, 2011] . The signal will be low at such

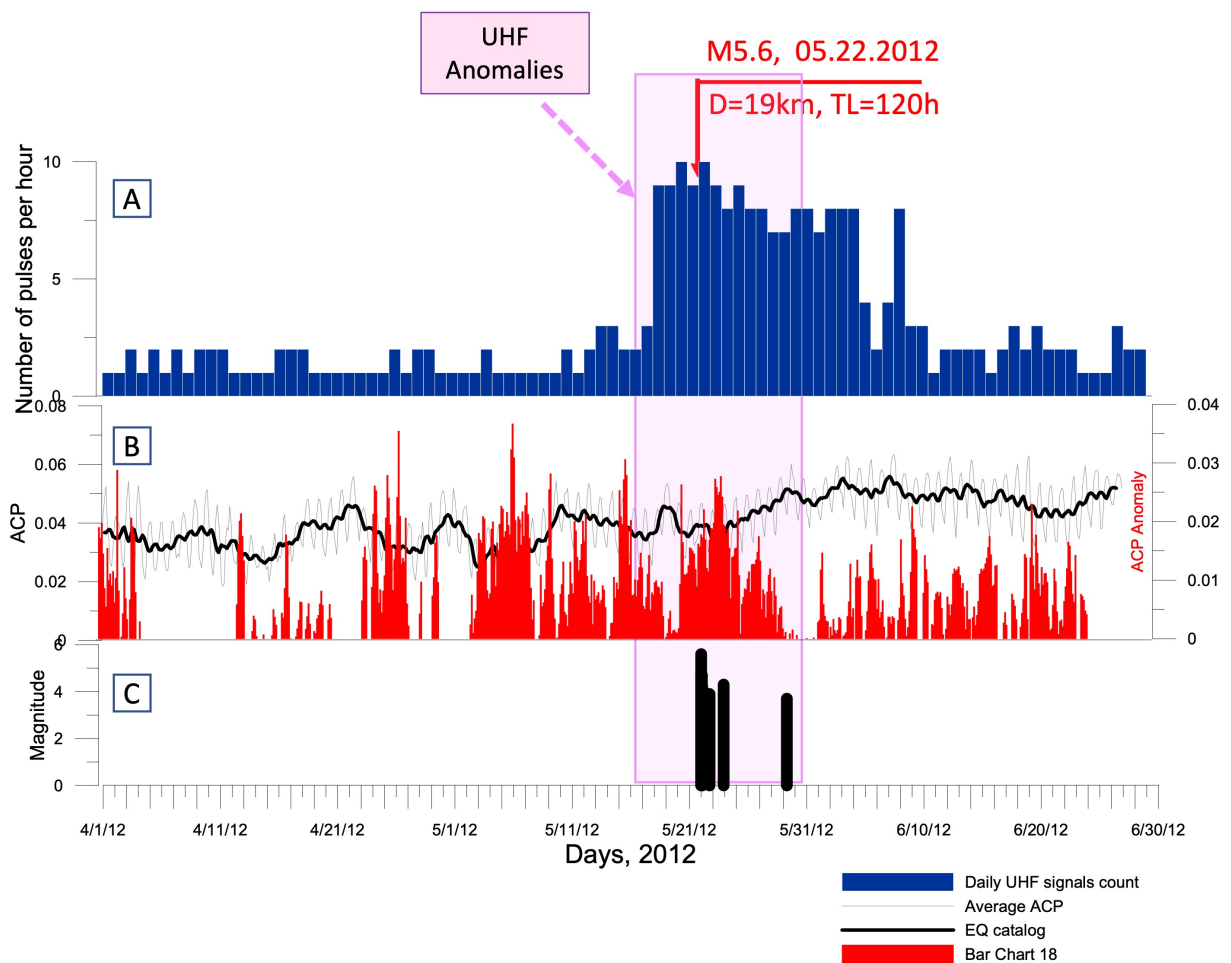


Figure 4. A: UHFV time-series of anomalous values before the M 5.8, May 22, 2012, Pernik, NW Bulgaria. The UHF anomalous pattern started on May 17, five days before the 2012 earthquake in Pernik (Bulgaria); B: ACP time series of average field (black) and anomalies level (red) based on the 2009-2012 definition period. C: The earthquake catalog data has been provided by EMSC.

a distance, and at 12-15 km, the expected will now be 0, i.e., the signal will be attenuated entirely. The estimating zone has a crucial role in the dynamic range of the amplified signal to monitor the significant enhancement of the existing standard receiver service MaxTelekom DSL 2.0.

3.2 M6.9 of May 24, 2014, in the Aegean Sea, Greece

The UHF monitoring presents the variations with time of the amplitude ratio input/output signal in mV/V (output/in-V/mV) averaged over a time interval. A DSL2.0 modem/router was used for the receiver with a main signal at 3.5 GHz. M6.9 of May 24, 2014, in the Aegean Sea, Greece, is the strongest magnitude we registered with our UHF systems in Bulgaria (Figure 5). We observed the anomalous patterns increase beginning about 38 days (912 hours) before the earthquake. The data on all graphs is BG time.

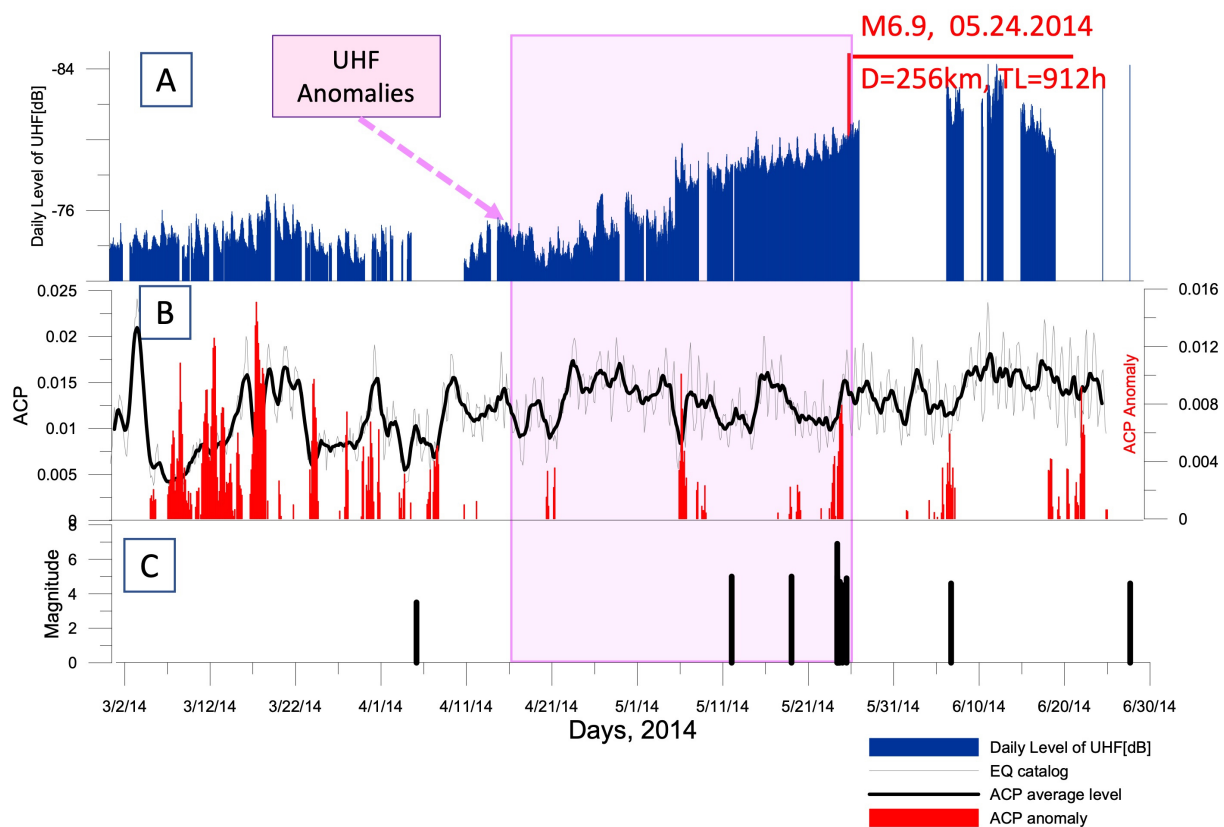


Figure 5. A: The variations with time of the amplitude ratio input/output signal in mV/V(output/in-V/mV) averaged over a time interval before the M6.9 of May 24, 2014, in the Aegean Sea, Greece. The UHF anomalous pattern started on April 21, 2014, about a month before the M6.9 event. B: ACP time series of average field (black) and anomalies level (red) based on the 2011-2014 definition period. C: The earthquake catalog data has been provided by EMSC.

3.3 M6.5 of Nov 17, 2015, Lefkada, Greece

UHF signals are tracked by the change in the frequency of pulses with a certain above-threshold amplitude with time (of the carrier frequency). VHF direct antennas in the range of 1.5-2.1 GHz are used, tracking a useful signal at 1.8 GHz (broadcast-upload signal – on LTE modems). Figure 6 illustrates VHF recording in two observation points – Mar and Most. The variations in the number of pulses of UHF above the threshold level (–50 dB) are shown in Figure 6A. The ACP time series of average field (blue) and anomalies level (red) based on the 2012-2015 definition period is Figure 6B, and the earthquake catalog data has been provided by EMSC (Figure 6C). The significant frequency increase occurred 12 days before the earthquake.

Modulation in the UHF signals caused by pre-earthquake processes

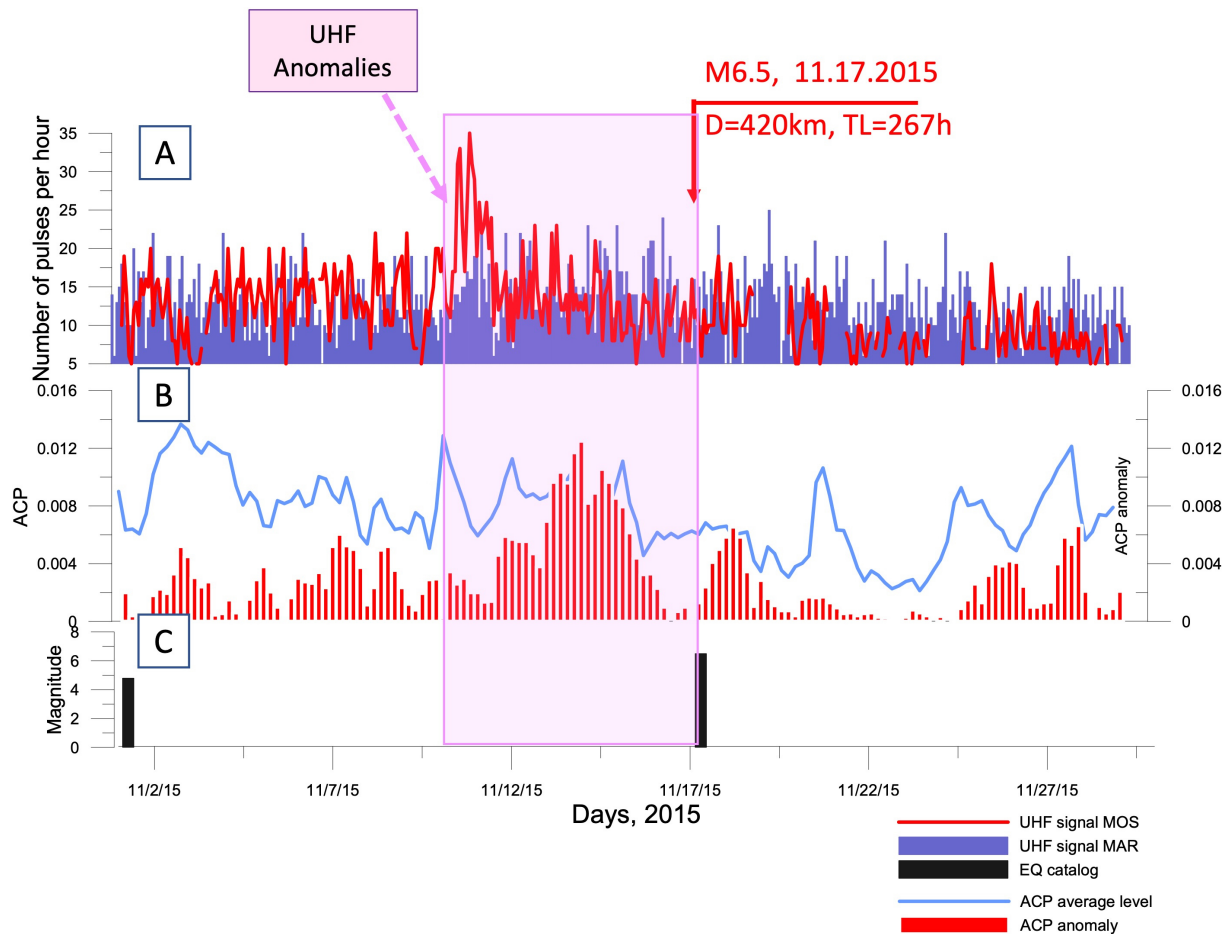


Figure 6. A: The variations in the number of pulses of UHF above the threshold level (-50 dB) are shown in the M6.5 of Nov 17, 2015, in Lefkada, Greece. B: ACP time series of average field (blue) and anomalies level (red) based on the 2012-2015 definition period. C: The earthquake catalog data has been provided by EMSC.

3.4 M6.3 of June 12, 2017, in Western Türkiye

VHF signals are tracked by the change in the frequency of pulses with a certain above-threshold amplitude with time (of the carrier frequency). A VHF direct antenna was used in the 1.5-2.1 GHz range, tracking a useful signal at 1.8 GHz (broadcast-upload signal – on an LTE modem). Figure 7A shows the variations in the number of pulses of UHF above the threshold level (-50 dB) are shown for Western Türkiye before the M6.3 of May 12, 2017, for one point of observation. The ACP time series of average field (blue) and anomalies level (red) based on the 2014-2017 definition period is compared with UHF (Figure 7B). The earthquake catalog was provided by EMSC (Figure 7C). The anomalous period of increased intensity started on May 19, 2017, and continued for 220 hours with many gaps (no data) between. The second period associated with the M6.3 of June 12, 2017, started on June 1st, 2017, for 10 days. The interruption in the graphs is due to a lack of data for technical reasons.

3.5 M5.0 of Jan 2, 2018, Northern Greece

The UHF signal can be traced through the change in the pulse frequency over the threshold amplitude with time (of the carrier frequency). Using the VHF direct antenna in the interval 1.5-2.1 GHz, a 1.8 GHz signal is traceable (the signal on the upload-upload is on the LTE modems) to two points on observation – Mar and Most. Figure 8 shows the variations in the number of pulses of UHF above the threshold level (-50 dB) in Northern Greece before M5.1 of Jan 2, 2018 (Figure 8A). The time series of average field (blue) and anomalies level (red) based on the 2014-2017 definition period (Figure 8B) and the earthquake catalog provided by EMSC (Figure 8C). The period to increase before the first M5.1 earthquake is 8 hours, and on the second from M5.0, about 48 hours (Figure 8).

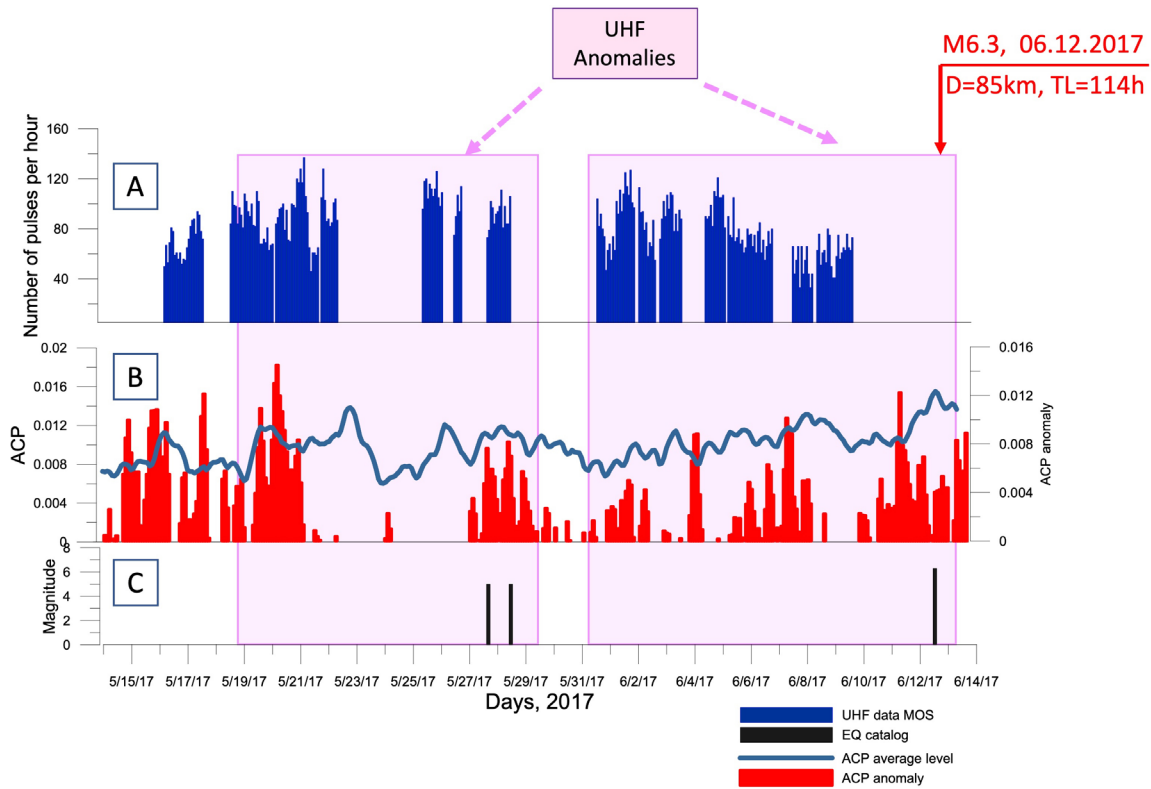


Figure 7. A: The variations in the number of pulses of UHF above the threshold level (-50 dB) are shown for Western Türkiye before the M6.3 of May 12, 2017. B: ACP time series of average field (blue) and anomalies level (red) based on the 2014-2017 definition period. C: The earthquake catalog was provided by EMSC.

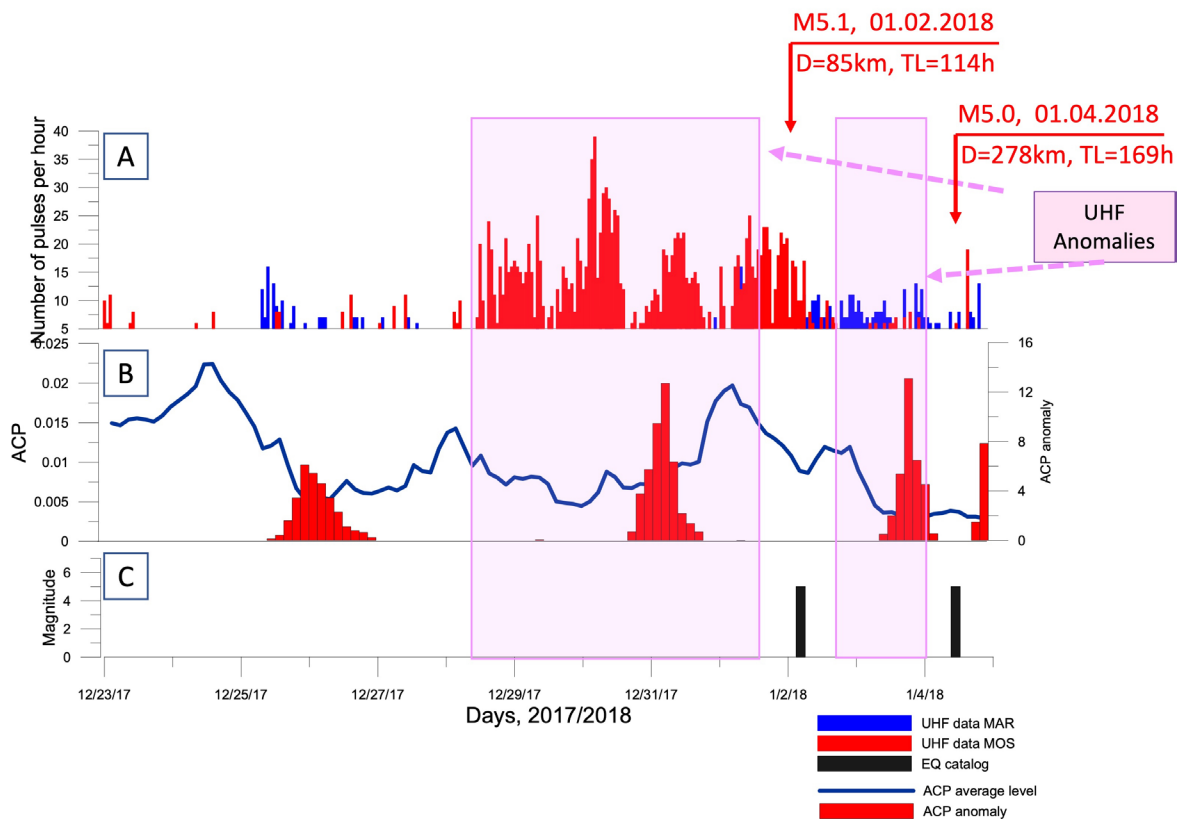


Figure 8. A: The variations in the number of pulses of UHF above the threshold level (-50 dB) are shown in Northern Greece before M5.1 of Jan 2, 2018; B: time series of average field (blue) and anomalies level (red) based on the 2014-2017 definition period. C: The earthquake catalog was provided by EMSC.

3.6 M4.1 Bulgaria and M5.1 in Albania August 2018

UHF signals are tracked by the change in the frequency of pulses with a certain above-threshold amplitude with time (of the carrier frequency). VHF direct antennas in the range of 1.5-2.1 GHz are used, tracking a useful signal at 1.8 GHz (broadcast-upload signal – on LTE modems). Figure 9 shows the results of observations in 2018 for two earthquakes – M5.1 in Albania on August 12 and M 4.1 on August 2 in Southern Bulgaria (Tables 1,3). The variations in the number of pulses of UHF above the threshold level (–50 dB) are shown for two observation points – Mar and Most (Figure 9A). The ACP average variation (blue curve) and anomaly values (red) for (2015-2018) are presented (Figure 9B). The earthquake catalog was provided by EMSC (Figure 9C). The anomalous period of increased intensity started on July 24, 2018 – 226 hours before M4.1 (9 days and 10 hours).

The UHF signals have three zones of activity.

- 1) July 24-26, 2018. This is the influence of a magnetic storm on observations. The anomaly is characterized by a significant amplitude but short duration in the temporal range.
- 2) July 29-August 1, 2018 This period is defined differently by anomalous values from both stations. The antenna of MOS (red color) is closer to the epicenter (50 km) and shows a typical anomaly of pulse variations starting 2-3 days before the earthquake. Teha antenna MAR shows an anomaly that starts together with MAS but subsides more quickly.
- 3) August 9-12, 2018 MOS shows a typical pre-seismic anomaly. MAR does not show an anomalous effect.

These two events are at different distances and seen at different angles to the receiver-antenna line. The MAR-MOS line is perpendicular to the epicenter-receiver line, while MOS-Tserovo is parallel to this line. In this way, they register various effects at the receiving stations. The effect of antenna MOS is stronger. This shows the need for a network placement of the observation antennas for optimal registration of the signals.

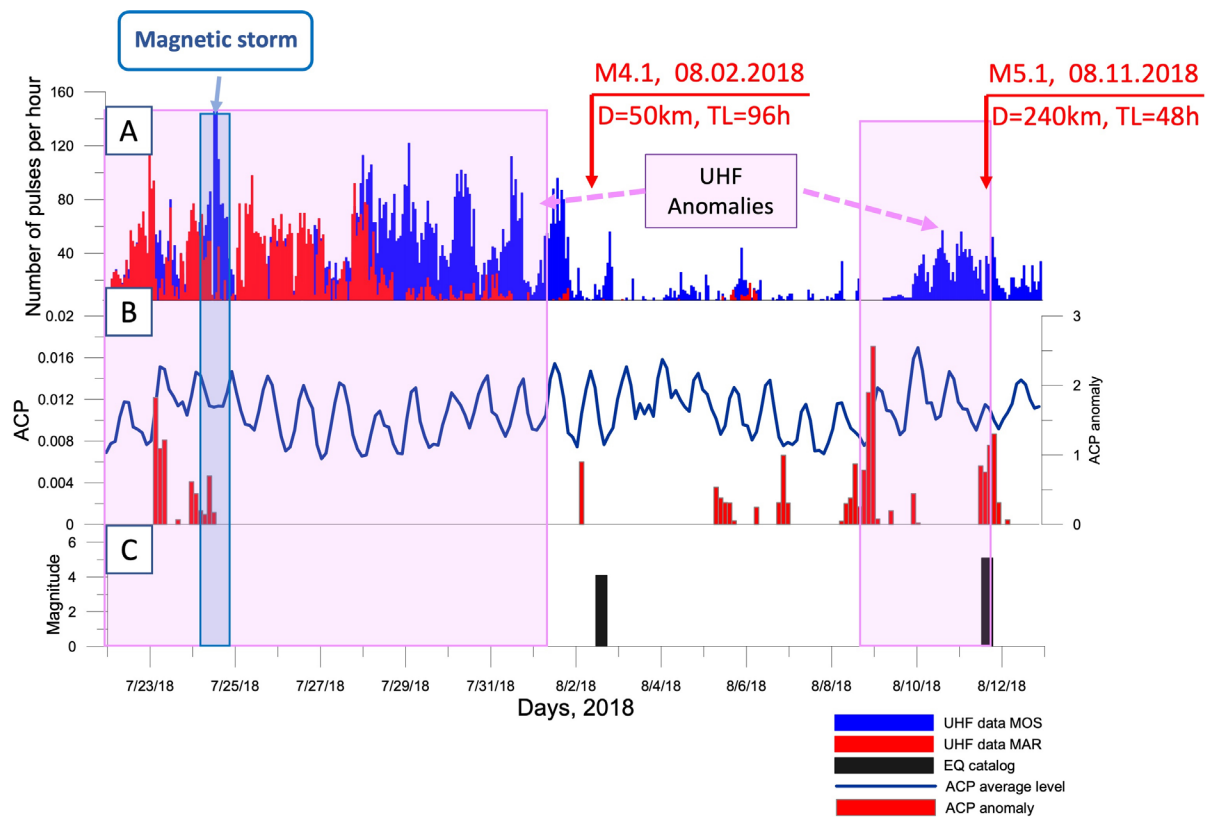


Figure 9. The results of observations in 2018 for two earthquakes – M5.1 in Albania on August 12 and M4.1 on August 2 in Southern Bulgaria (Tables 1, 3). A: The variations in the number of pulses of UHF above the threshold level (–50 dB) are shown; B: ACP average variation (blue curve) and anomaly values (red) for (2015-2018) are presented. C: The earthquake catalog was provided by EMSC.

Region	Date	Time	Long	Lat	Depth [km]	M	Focal mechanism	Distance to UHF receiver [km]	Freq Range [GHz]	Time lag [h]	Amplitude change [dBm]
CENTRAL ALBANIA	2018-08-11	15:38:34	41.59	20.21	10	mb = 5.1	strike-slip (right lateral)	278	1.8	321	95
SOUTH-EAST MONTENEGRO	2018-01-04	10:46:10	42.67	19.88	7	mb = 5	nor/strike-slip	278	1.8	169	39
NORTHERN GREECE	2018-01-02	04:24:16	41.22	22.86	6	mb = 5	oblique normal	85	1.8	114	39
NEAR WESTERN TÜRKIYE	2017-06-12	2:28:37	38.85	26.31	9	Mw = 6.3	oblique normal	437	1.8	560	42
WESTERN TÜRKIYE	2017-05-28	11:04:59.8	38.73	27.78	9	mb = 5.0	normal	533	1.8	187	42
WESTERN TÜRKIYE	2017-05-27	15:53:23.9	38.72	27.83	13	mb = 5	normal	533	1.8	167	42
GREECE-near Lefkada	2015-11-17	07:10:08	38.76	20.45	10	Mw = 6.5	strike-slip	420	1.8	267	34
WESTERN TÜRKIYE	2014-05-24	09:31:18	40.4	26.28	2	mb = 5	no info	313	3.5/AVI	2000	10
AEGEAN SEA	2014-05-24	09:25:02	40.29	25.4	27	Mw = 6.9	strike-slip (right)	266	3.5/AVI	2000	10
CENTRAL ALBANIA	2014-05-19	00:59:20	40.94	19.81	10	Mw = 5	strike-slip/dip-slip	296	3.5/AVI	1890	10
SOUTHERN ALBANIA	2014-05-12	00:54:33	39.76	20.27	4	mb = 5	dip-slip/strike-slip	340	3.5/AVI	1750	10
BULGARIA-near Sofia	2012-05-22	00:00:33	42.66	23.01	10	Mw = 5.6	normal	19	3.5	120	7.5

Table 3. The extended earthquake catalog (source EMSC catalog) for the period of 2012–2018, which was analyzed with the UHF observations and shown in Figure 1 and Table 1.

4. Discussion

The mechanism of this phenomenon proposed by Hayakawa et al. [2007] is due to increased gas emanation, surface temperature, groundwater lifting, and gas emanation, leading to a change in the atmospheric refraction index. Initially, the gas emanation concept concerning the pre-earthquake process was proposed by Pulinets et al. [1997], who described how gas emanation and radon and metallic aerosol emanate and form an atmospheric electric field. Most likely, the observed increase in the intensity is a direct result of the change in the atmospheric properties in the ABL triggered by the intensification of radon and other gases released, which leads to a change in lower atmosphere conductivity, already suggested by LAIC concept [Pulinets and Ouzounov, 2011].

The main principle of the LAIC concept, shown as a flowchart in Figure 10, considers both wave and electromagnetic information transmission channels from the ground up to the atmosphere/ionosphere. More details about the LAIC concept can be found in Pulinets and Ouzounov [2011] and the latest updates [Ouzounov et al., 2018; Pulinets et al., 2018; 2022]. Naturally, we know that an earthquake results from tectonic activity when, due to deformation created by the interaction of tectonic plates in some places, stress exceeds the material strength [Scholz, 1990]. Just at the last stage of earthquake preparation, we observe the activation of faults within the area of earthquake preparation, which leads to the increased emanation of gases such as carbon dioxide, methane, hydrogen, and helium, including radon [Khilyuk et al., 2000, Aumento, 2002] (rectangle 1). Radon, due to its radioactivity, produces air ionization [Harrison et al., 2010] (rectangle 2). The so-called Ion Induced Nucleation process starts if its intensity is strong enough [Laakso et al., 2002] (rectangle 3). This process leads to the formation of large-charged ion clusters consisting of the charged core ion with the envelope of water molecules that attach to the ions due to their high dipole moment [Sekimoto and Takayama, 2007]. Ion Induced Nucleation is essentially a nonlinear process because it is a catalytic exothermic process with simultaneously coexisting two aggregation phase states of the water: condensed and vapor.

Modulation in the UHF signals caused by pre-earthquake processes

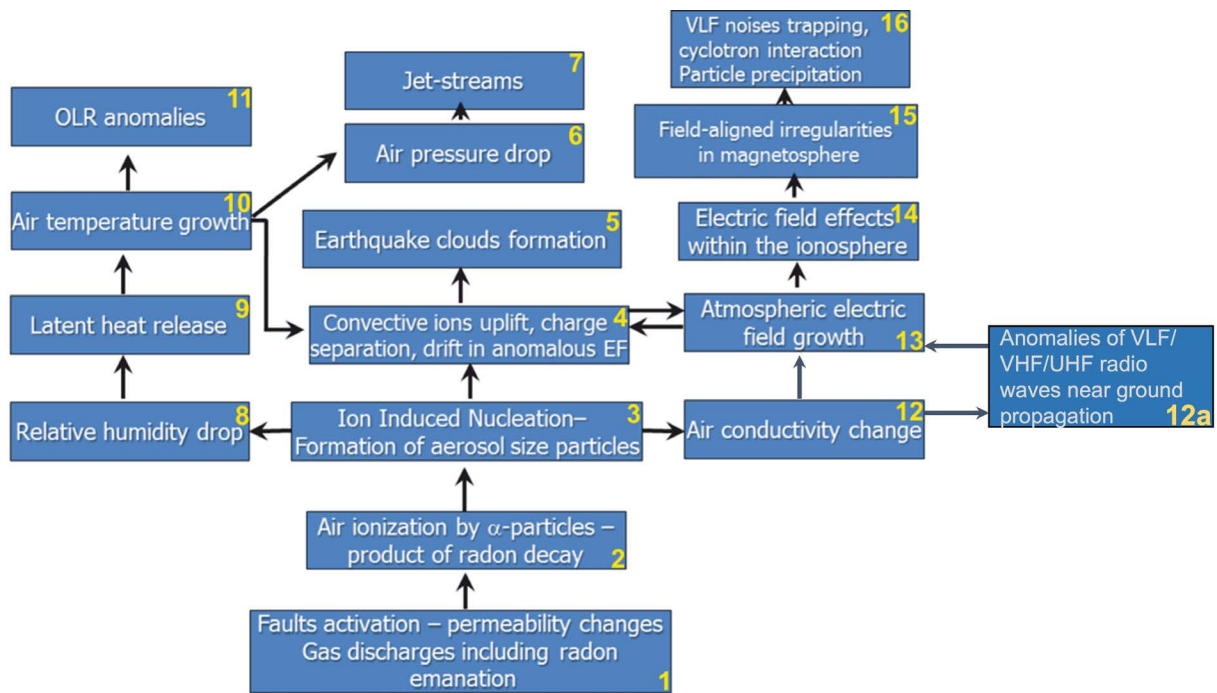


Figure 10. Flow-chart of the LAIC concept.

Relative air humidity drops because of water vapor condensation on ions (rectangle 8), the latent heat release rises (rectangle 9), and air temperature grows (rectangle 10). It is well known from meteorology that sharp air humidity drops accompany air temperature growth. The additional heat flux due to the latent heat release could be registered in the long wave part of the infrared emission within the transparency window of the atmosphere 8-14 μ from the satellites (rectangle 11). The air growth creates thermal convection, raising the newly formed nucleus of condensation (rectangle 4), which reaches the altitude of the cloud formation and makes the earthquake type of specific cloud structures called Cloud Anomalies (CA) (rectangle 5). The jet streams to the position of the thermal anomaly will be formed (rectangle 6).

At this point, we describe the electromagnetic effects (rectangles 12-16). The small and medium-sized ions increase the boundary layer's electric conductivity, while the large ones if their concentration is high enough, will essentially decrease it (rectangle 12). Considering the Global Electric Circuit conception [Pulinets and Davidenko 2014], we can expect in the case of the boundary layer conductivity to drop the increase of the vertical electric field gradient (rectangle 13), which will change the ionosphere potential about the ground over the earthquake preparation area. Some large-scale plasma irregularities in the ionosphere will be formed (rectangle 14). These irregularities will form the modified magnetospheric ducts (rectangle 15). These ducts will trap the VLF emission inside the modified magnetospheric tube, creating increased VLF noises within the modified tube (rectangle 16). The radio wave propagation that we consider in this paper has three versions in the LAIC concept: anomalies of sub-ionospheric propagation of the VLF emissions from navigational transmitters [Rozhnoi et al., 2004] and over-horizon propagation of VHF waves [Moriya et al., 2010] and UHF/VHF observation within the ABL layer [Ouzounov et al., 2016]. We consider all the cases because of the boundary layer conductivity modification (rectangle 12). In this direction, we will develop a featured physical mechanism by adding rectangle 12a titled "anomalies of VLF and VHF radio waves near ground propagation."

The heated air masses over the faults will rise, carrying with them the charged ion clusters serving as nucleation centers. Elevated charged clusters will gain more and more water molecules, and one may expect the formation of a cloud over the fault.

The influence of meteorological factors on VHF propagation could be considered pre-EQ consequence. ACP is also a meteorological factor, and the ducts should be considered the following: The distribution of large ion clusters in the boundary layer is heterogeneous. We should remember that the radon emanates from the active tectonic fault, representing some linear structure. The ACP repeats the shape of these faults, forming the proto clouds in the lower atmosphere, forming the so-called linear earthquake clouds shown on Figure 11 [Morozova et al., 2020].

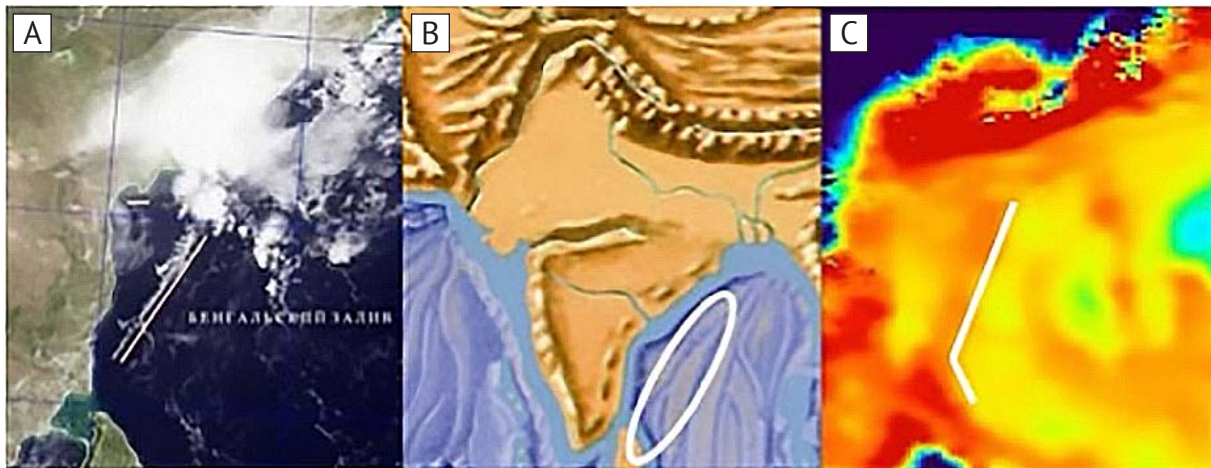


Figure 11. A: Cloud ridge in the Bay of Bengal 24.04.2015; B: tectonic fault at the bottom of the Bay of Bengal, coinciding with the position of the cloud bank (encircled with white); C: quasi-meridional structure of high humidity. Coinciding of the cloud bank (marked with a white line) [Morozova et al., 2020].

The humidity distribution is at the level of 100 m over the ocean surface. So, these meteorological anomalies formed by the ionization process in the near ground layer of the atmosphere create anomalous channels for the VHF and UHF wave propagation. The linear cloud structure concept over the active tectonic fault has also been discussed in [Liperovsky et al., 2005]. They use the idea of radon and aerosol emanations over the active tectonic fault described first in [Pulinets et al., 1997]. But more recent studies demonstrated that there is no evident aerosol emanation over tectonic faults, and the complex ions clusters play the role of centers of the water vapor condensation, simultaneously growing to the aerosol size of the order of several microns as it was described in [Pulinets and Ouzounov, 2011]. The core of the LAIC concept related to the earthquake preparation process often needs to be better understood. Radon and ionization do not produce any energy; the energy is released due to the condensation of the water vapor on ions and the consequent release of the latent heat contained in the air-water vapor. Although we only use air temperature and relative humidity to calculate ACP within the ABL in this paper, it reflects the effects of radon ionization on the atmosphere, changing its thermodynamic and electric properties.

5. Conclusion

We observed UHF and SHF phenomena associated with the natural enhancement of the intensity of 1.8-3.5 GHz signals (no change in the transmitting level) due to electric and electrochemical changes in the atmosphere over the regions of ongoing earthquake preparation. We have established monitoring of the UHF range of LTE about earthquake activities in Southwest Bulgaria (NE Europe) since August 2013, and our initial field observations indicate the following findings:

- Stable effects of a systematic increase in intensity (with different speeds) related to regional seismicity in the LTE range 1.8-1.9 GHz were registered. Weak and moderate earthquakes ($M2-4.5$) create a slow change (hours, days) in intensity level. Anomalous signals appear as impulse oscillations with a maximum (1-4 days before the earthquakes) and a fading amplitude modulation hours before the earthquakes.
- Since 2013, with WiMAX and LTE internet signals transmission technologies received with VHF antennas, we have recorded pre-earthquake signatures associated with several strong earthquakes in the Balkan region: $M5.6$ on May 22, 2012 (Sofia, Bulgaria), $M6.4$ on October 12, 2013 (Crete, Greece), and $M6.9$ on May 24, 2014, Aegean Sea and more moderate seismicity events [Ouzounov et al. 2016; 2017; 2019; 2021]. We are registering an effect of a systematic increase (with a different rate) at the range of 1.8-3.5 GHz associated with the regional seismicity and no significant intensified modulation with an absence of major seismicity in the region.
- The UHF and SHF observations have an excellent potential for proving new information about the state of development in the ABL before and during the earthquake activities if they are transformed into network observations and combined with other similar measurements (radon, GPS, electrical field).

Modulation in the UHF signals caused by pre-earthquake processes

- The intensity change depends on several factors: 1) the configuration of the receiver/transmitter, 2) the distance to the earthquake events, and 3) the magnitude scale. Such a type of variation is not observed with a lack of ongoing seismicity.
- Most likely, the observed increase in the intensity is a direct result of the change in the atmospheric conductivity near the ABL suggested by the LAIC concept. A dedicated network of several VHF receivers is needed to validate this phenomenon comprehensively.
- The spatial characteristics of pre-earthquake UHF and SHF anomalies were associated with the large area but inside the EPZ estimated by Dobrovolsky-Bowman.

Data Availability Statement. The datasets generated for this study are available on request to the corresponding author.

Acknowledgments. Dimitar Ouzounov thanks the Institute of ECHO at Chapman University, CA, USA, for their support. The authors also thank the US Geological Survey and European–Mediterranean Seismological Centre for the earthquake information services and data. Special thanks to Ertha Systems and Act Sofia for supporting these observations. This research is partially supported by the Bulgarian National Fund for Scientific Research, contract No. Д 14/1 from 11.12.2017 and by the project “Multi-instrument Space-Borne Observations and Validation of the Physical Model of the Lithosphere-Atmosphere Ionosphere-Magnetosphere Coupling,” International Space Science Institute (Bern).

References

- Aumento, F. (2002). Radon tides on an active volcanic island: Terceira, Azores, *Geofísica Internacional*, 41, N. 4, 499-505.
- Bowman, D.D., G. Ouillon, C.G. Sammis, A. Sornette and D. Sornette (1998). An observation test of the critical earthquake concept, *J. Geophys. Res.*, 103, 24359-24372.
- Dobrev, N. (2011). 3D monitoring of active fault structures in the Krupnik-Kresna seismic zone, SW Bulgaria. *Acta Geodynamica et Geomaterialia*, 8, 4, 164, 377-388.
- Dobrovolsky, I.P., S.I. Zubkov and V.I. Myachkin (1979). Estimation of the size of earthquake preparation zones, *Pure Appl. Geophys.*, 117, 5, 1025-1044.
- Fujiwara, H., M. Kamogawa, M. Ikeda, J.Y. Liu, H. Sakata, Y.I. Chen, H. Ofuruton, S. Muramatsu, Y.J. Chuo and Y.H. Ohtsuki (2004). Atmo spheric anomalies observed during earthquake occurrences, *Geophys. Res. Lett.*, 31, L17110.
- Fukumoto, Y., M. Hayakawa and H. Yasuda (2001). Investigation of over-horizon VHF radio signals associated with earthquakes, *Nat. Hazards Earth Syst. Sci.*, 1, 107-112.
- Harrison R.G., K.L. Aplin and M.J. Rycroft (2010). Atmospheric electricity coupling between earthquake regions and the ionosphere, *JASTP*, 72, 376-381.
- Hayakawa, M., V.V. Surkov, Y. Fukumoto and N. Yonaiguchi (2007). Characteristics of VHF over-horizon signals possibly related to impending earthquakes and a mechanism of seismo-atmospheric perturbations, *J. Atmos. Solar-Terr. Phys.*, 69, 1057-1062.
- Hayakawa M. (2018). Earthquake Precursor Studies in Japan, In the Book: Pre-Earthquake Processes: A Multidisciplinary Approach to Earthquake Prediction Studies, (Eds: Ouzounov, Pulinets, Hattori Taylor) *Geophysical Monograph* 234, 2018 American Geophysical Union. John Wiley & Sons, Inc, 7-18.
- Kapiris, P., J. Polygiannakis, K. Nomicos and K. Eftaxias (2002). VHF electromagnetic evidence of the underlying pre-seismic critical stage, *Earth Planets Space*, 54, 1237-1246.
- Keilis-Borok V.I. and V.G. Kossobokov (1990). Premonitory activation of earthquake flow, algorithm, M8, *Phys. Earth Planet. Inter.*, 61, 73-83.
- Khilyuk, L.F., G.V. Chillingar, J.O. Robertson Jr. and B. Endres (2000). Gas migration. Events preceding earthquakes. Gulf Publishing Company, Houston, Texas. 390.
- Knyazeva, H.N. and S.P. Kurdyumov (2008). Synergetics: New Universalism or Natural Philosophy of the Age of Post-Nonclassical Science, *Dialogue and Universalism*, 11-12, 39-61.

- Kotzev, V., R. Nakov, Tz. Georgiev, B.C. Burchfiel and R.W. King (2006). Crustal motion and strain accumulation in western Bulgaria. *Tectonophysics*, 413, 127-145.
- Kushida, Y. and R. Kushida (2002). Possibility of earthquake forecast by radio observations in the VHF band, *J. Atmos. Electr.*, 22, 239-255.
- Laakso L., J.M. Mäkelä, L. Pirjola and M. Kulmala (2002). Model studies on ion-induced nucleation in the atmosphere, *J. Geophys. Res.*, 107, D20, 4427.
- Liperovsky, V.A., C-V. Meister, E.V. Liperovskaya, V.F. Davidov and V.V. Bogdanov (2005). On the possible influence of radon and aerosol injection on the atmosphere and ionosphere before earthquakes, *Nat. Hazard*, 5, 783-789.
- McClusky, S., S. Balassanian, A. Barka, C. Demir, S. Erginav, I. Georgiev, O. Gurkan, M. Hamburger, K. Hurst, H. Kahle, K. Kastens, G. Kekelidze, R. King, V. Kotzev, O. Lenk, S. Mahmoud, A. Mishin, M. Nadarya, A. Ouzounis, D. Paradisis, Y. Peter, M. Prilepin, R. Reilinger, I. Sanli, H. Seeger, A. Tealeb, M.N. Toksoz and G. Veis (2000). Global Positioning System constraints on plate kinematics and dynamics in the eastern Mediterranean and Caucasus, *J. Geophys. Res.* 105, 5695-5719.
- Moriya, T., T. Mogi and M. Takada (2010). Anomalous pre-seismic transmission of VHF-band radio waves resulting from large earthquakes, and its statistical relationship to magnitude of impending earthquakes, *Geophys. J. Int.*, 180,858-870.
- Morozova, L.I., A.V. Nikolaev and S.A. Pulinets (2020). Cloud anomalies and earthquakes, *Geology and Geophysics of Russian South*, 10, 3, 57-78.
- Ouzounov, D., S. Velichkova-Yotsova and S. Pulinets (2016). Anomalous variation in the wireless signals propagation associated with earthquake preparation processes, *Geophys. Res. Abs.*, 18, EGU2016-3522.
- Ouzounov, D., S. Velichkova-Yotsova, S. Pulinets, A. Velez and N. Hatzopoulos (2017). Modulations in VHF Wireless Signals Linked to Pre-earthquake Processes, 32nd URSI GASS, Montreal, 19-26 August.
- Ouzounov, D., S. Pulinets, K. Hattori and P. Taylor (2018). Pre-Earthquake Processes: A Multidisciplinary Approach to Earthquake Prediction Studies, *Geophysical Monograph 234*, First Edition, American Geophysical Union, John Wiley & Sons, Inc, 384.
- Ouzounov, D., S. Velichkova-Yotsova and S. Pulinets (2019). Modulation of Wireless VHF Signals Associated with Remote Earthquakes, 27th IUGG General Assembly Montreal, Canada, S15, 137.
- Ouzounov, D., S. Velichkova and E. Botev (2021). Modulation in VHF Wireless Signals Associated With Pre-earthquake Processes. Case Studies for the Balkans European Association of Geoscientists and Engineers; Conference Proceedings, 11th Congress of the Balkan Geophysical Society, Oct 2021, 2021, 1-5.
- Pulinets, S.A., V.A. Alekseev, A.D. Legen'ka and V.V. Khagai (1997). Radon and metallic aerosols emanation before strong earthquakes and their role in atmosphere and ionosphere modification, *Adv. Space Res.*, 20, 2173-2176.
- Pulinets, S.A., D. Ouzounov, L. Ciraolo, R. Singh, G. Cervone, A. Leyva, M. Dunajacka, A.V. Karelin, K.A. Boyarchuk and A. Kotsarenko (2006). Thermal, atmospheric and ionospheric anomalies around the time of the Colima M7.8 earthquake of 21 January 2003, *Annales Geophysicae*, 24, 835-849.
- Pulinets, S. and D. Ouzounov (2011). Lithosphere-Atmosphere-Ionosphere Coupling (LAIC) model – An unified concept for earthquake precursors validation, *J. Asian Earth Sci.*, 41, 371-382.
- Pulinets, S. and D. Davidenko (2014). Ionospheric precursors of earthquakes and global electric circuit, *Adv. Space Res.*, 53, 709-7231, 371-382.
- Pulinets, S.A., D.P. Ouzounov, A.V. Karelin and D.V. Davidenko (2015). Physical bases of the generation of short-term earthquake precursors: A complex model of ionization-induced geophysical processes in the lithosphere-atmosphere-ionosphere-magnetosphere system, *Geomagn. Aeron.*, 55, 521-38.
- Pulinets, S. and D. Ouzounov (2018). The Possibility of Earthquake Forecasting: Learning from nature, Institute of Physics Books, IOP Publishing, 168.
- Pulinets, S., D. Ouzounov, A. Karelin and K. Boyarchuk (2022). *Earthquake Precursors in the Atmosphere and Ionosphere: New Concepts*, Springer, ISBN-940242170X, 312.
- Rozhnoi, A., M.S. Solovieva, O.A. Molchanov and M. Hayakawa (2004). Middle latitude LF (40 kHz) phase variations associated with earthquakes for quiet and disturbed geomagnetic conditions// *Phys. Chem. Earth.*, 29, 589-598.
- Scholz, C.H. (1990). *The mechanics of earthquakes and faulting*, Cambridge University Press, Cambridge
- Sekimoto, K. and M. Takayama (2007). Influence of needle voltage on the formation of negative core ions using atmospheric pressure corona discharge in air, *Int. J. Mass Spectro.*, 261, 1, 38-44.
- Uyeda, S. and T. Nagao (2018). International Cooperation in Pre-Earthquake Studies: History and New Directions, In the Book: *Pre-Earthquake Processes: A Multidisciplinary Approach to Earthquake Prediction Studies*

Modulation in the UHF signals caused by pre-earthquake processes

(Eds: Ouzounov, Pulinets, Hattori Taylor) Geophysical Monograph 234, 2018 American Geophysical Union. John Wiley & Sons, Inc, 3-6.

Yasuda, Y., Y. Ida, T. Goto and M. Hayakawa (2009). Interferometric direction finding of over-horizon VHF transmitter signals and natural VHF radio emissions possibly associated with earthquakes, *Radio Sci.*, 44, RS2009.

Yonaiguchi, N., Y. Ida and M. Hayakawa (2007). On the statistical correlation of over-horizon VHF signals with meteorological radio ducting and seismicity, *J. Atmos. Solar-Terr. Phys.*, 69, 661-674.

***CORRESPONDING AUTHOR: Dimitar OUZOUNOV,**

Institute for Earth, Computing, Human and Observing (Institute for ECHO), Chapman University, Orange, CA, USA

e-mail: dim.ouzounov@gmail.com